Application of non-Newtonian models to thin film flow

T. G. Myers
Department of Mathematics and Applied Mathematics, University of Cape Town, Rondebosch 7701, South Africa
(Received 29 June 2005; published 7 December 2005)

The paper describes an investigation into the use of lubrication models on thin film flow. Power law, Ellis, and Carreau models are compared for free surface flow and flow within a channel. It is shown that the Ellis law (or a slight modification) can give very similar viscosity curves to Carreau. The three models are then compared for thin film flow with a constant height free surface. For low shear rates the power law model can give very inaccurate predictions. Having shown Carreau and Ellis may produce similar results we then study flow in a channel for Ellis and power law fluids. Again the power law can give inaccurate results due to the high viscosity around the turning point for the velocity. Finally, we briefly describe the modification to include surface tension in the free surface flow model.

DOI: 10.1103/PhysRevE.72.066302 PACS number(s): 47.50.+d, 47.15.Gf, 47.60.+i

I. INTRODUCTION

The flow of a thin layer of Newtonian fluid has been the subject of intense investigation for many years. One reason for this interest is the wide variety of applications of such flows, both natural and industrial (see [1,2] for example). However, there are many practical applications where the fluid is non-Newtonian. They may exhibit a nonlinear stress-strain relation or have a nonzero yield stress. In this paper we will focus on fluids with a nonlinear stress-strain relation. Most fluids that do not have a yield stress exhibit Newtonian behavior at very high and very low shear rates and are shear thinning at moderate shear rates. Most polymeric fluids fit this description, as do certain suspensions [3–5]. These fluids are often referred to as having structural viscosity since the change in viscosity may be associated with a breakdown of the structure which subsequently recovers upon removal of the stress. Mud, blood, ice, and fluidized beds have also been modeled as having some form of structural viscosity [6–9].

In general polymeric fluids show four distinct viscosity regimes when subject to shear stress. At very low shear rates they behave as a Newtonian fluid; as the shear increases the behavior starts to become nonlinear, after a further increase it moves into the regime where the viscosity can be modeled by a power law relation. Finally, at very high shear rates the behavior becomes Newtonian once more [3,5,10].

In many industrial applications, such as injection molding or extrusion, fluids are subjected to high shear rates (in the range $[1,10^4]$ s^{-1} [4]) and so are well described by the power law model. However, when a fluid is subject to a range of shears including very low values, a different model must be used. Obviously, there are many of these, however, commonly used ones include Carreau, Cross, and Ellis (see [3,4] for example). The power law, Carreau, and Cross models express viscosity in terms of shear rate and have two, four, and four free parameters, respectively. The Ellis model expresses viscosity in terms of shear stress and has three parameters. All three of Carreau, Cross, and Ellis can describe the low shear Newtonian plateau. Carreau and Cross can also model the high shear Newtonian region. However, the high shear viscosity is usually significantly less than the low shear value and is frequently neglected, hence, the final three models, in practice, usually involve the same number of free parameters.

Despite the fact that it is well known that the power law model is only meant to apply at large shear rates, it is frequently used for flows where the shear stress becomes zero. In this limit the power law model predicts infinite fluid viscosity. In particular it has been used in studies of free surface flow (subject to a zero shear boundary condition) [9,11–21], hence the viscosity becomes infinite at the free surface. In pipe flows and metered coating the velocity is fixed at the walls and generally reaches a maximum within the flow, hence the velocity gradient (and therefore shear stress) becomes zero within the flow [22–24]. Other objections to the power law model include the fact that one of the constants has rather strange dimensions (dependent on the other constant) and the constants determined from one flow system may be different from those obtained from another flow system, with the same fluid [10]. Presumably the main reason for retaining the power law model for low shears is that it leads to an attractive mathematical model. This is pointed out in [4, pp. 266, 267] as follows, "Although the limitations of [the power law model] are well known, it continues to be used as a starting point for theoreticians to keep the mathematical complexity at a tractable level." They go on to point out that the power law model has been demonstrated to be inadequate when modeling creeping flow around a rigid sphere. In Matsuhisa and Bird [10] a number of applications where the power law model has proved inadequate are detailed.

Spin coating is a classic example where the coating fluids are typically non-Newtonian. The standard Newtonian solution for fluid flow on a spinning disk was given by Emslie *et al.* [25]. Their model had a dominant balance between centrifugal driven motion and viscous resistance of the fluid. One conclusion they drew was that an initially uniform layer remained uniform after centrifugation. Acrivos *et al.* [11] extended this work to include power law behavior of the fluid and demonstrated that a uniform film loses its uniformity. In fact the results showed that fluid near the center remained stationary and so formed a peak (contrary to experimental evidence). The amount of stuck fluid increased as the power law exponent n was decreased, an obvious consequence of the viscosity tending to infinity. Subsequently,

Jenekhe and Schuldt [26] demonstrated that this behavior was a consequence of applying the power law model at low shear rates. They solved the problem numerically, using a Carreau fluid model, and showed that a uniform film decreased almost uniformly. They concluded that power law fluids were unsuitable for modeling axisymmetric free surface flows.

So, there is clear evidence that power law fluids are inappropriate for certain low shear rate flows. It therefore seems reasonable to investigate whether this type of model can provide physically realistic results for thin film free surface flows on a fixed substrate.

In the following work we compare power law, Carreau, and Ellis models. We commence with an investigation of gravity driven flow down an inclined plane, where the free surface has a fixed height. This simple situation means that we can neglect any modulus signs that appear in the constitutive equations (since the velocity gradient is always positive) and we can therefore focus on how well each model works and under what conditions it is appropriate to use the model. We neglect the Cross model since this gives very similar results to Carreau.

The advantage of the Ellis model over Carreau is that, in the case of a film with one free surface, an explicit expression for the film height may be obtained. For flow in a channel a relation between the flux and pressure gradient may be obtained. Hence analytical progress may be made with the Ellis model. One objection to the Ellis model is that for certain fluids it may underpredict the viscosity in the low shear transition region from power law to Newtonian behavior [27,28]. However, for many fluids it does show good agreement, within 5% of experimental data, for over three decades of shear stress variation [10]. Throughout this paper we will assume that the Carreau model provides the best fit to experimental data. This may not be the case; the Ellis model may be better for certain fluids, however we do require a benchmark model for comparison purposes.

In the following section we demonstrate that the Ellis model (or a slight variant) and the Carreau model can be made to give virtually identical results for a wide range of shear rates for all the fluids examined, hence in subsequent sections we neglect the Carreau model. The power law model is shown to work well for relatively thick films, but results diverge as the film becomes very thin. In the final section we briefly demonstrate how the equations may be modified to deal with thin film flow including the effect of surface tension.

II. VISCOSITY MODELS

In this section we describe the use of the three viscosity laws used in the subsequent analysis. We then go on to compare the models for five different fluids.

A. Power law

The standard power law model describes the viscosity by

$$\eta_p = K|\dot{\gamma}|^{n_p-1}, \tag{1}$$

where $\dot{\gamma}$ is the shear rate. In the case of two-dimensional thin film flow, as will be considered in the following analysis, we may set $\dot{\gamma}=u_z$. If $n_p<1$, the fluid is pseudoplastic or shear thinning. If $n_p>1$, it is dilatant or shear thickening. Obviously, when $n_p<1$, as $\dot{\gamma}\to 0$ the viscosity tends to infinity. For $n_p>1$ the viscosity tends to zero as $\dot{\gamma}\to 0$.

B. Carreau model

The Carreau model is typically written in terms of four parameters

$$\eta_c = \eta_\infty + (\eta_0 - \eta_\infty)[1+\lambda^2\dot{\gamma}^2]^{(n_c-1)/2}, \tag{2}$$

where η_0, η_∞ are the limiting viscosities at high and low shear rates. The high shear viscosity is generally associated with a breakdown of the fluid and is frequently set to zero, see [29], [4, p. 267]. When a value for η_∞ is quoted it is always significantly less that η_0; for example, for 7% aluminum soap in decalin and m-cresol (hereafter referred to as aluminum soap) $\eta_\infty=0.01$ Pa s $\approx \eta_0/900$ [3], and for blood $\eta_\infty=0.0345\approx\eta_0/16$ [7]. In the following we will follow standard practice and neglect η_∞. The zero shear viscosity, for solutions, is usually taken as the viscosity of the carrier fluid.

In general the Cross model, which also has four parameters, yields very similar results to the Carreau model.

C. Ellis model

The Ellis model is written in terms of shear stress

$$\frac{1}{\eta} = \frac{1}{\eta_0}\left(1+\left|\frac{\tau}{\tau_{1/2}}\right|^{\alpha-1}\right), \tag{3}$$

where η_0 is the viscosity at zero shear and $\tau_{1/2}$ is the shear stress at which the viscosity is $\eta_0/2$. This model cannot predict the second Newtonian plateau, however, as stated this is usually not of interest and particularly not for this investigation where it is the low shear region that is of primary interest.

D. Experimental data

In Table I we give examples of the parameters for each model for five fluids. The data show a wide spread in the viscosities at zero shear, from 4×10^6 to 0.056 Pa s. There is also a good variation in the experimental data provided, i.e., some authors quote only Carreau parameters and we infer the others or vice versa.

The power law, Carreau, and Ellis parameters for molten polystyrene are taken from [4, pp. 966–968]. Only the Carreau parameters for 7% aluminum soap in decalin and m-cresol are given in [3, p. 210]. We obtain the power law parameters by considering just the shear thinning region, then we can set $n_p=n_c$ and $K=\eta_0\lambda^{n-1}$; these are the values shown in the table. The Ellis model parameters are obtained by curve fitting. However, this is not a difficult task. Although the model has three parameters, two are simple to obtain. The viscosity η_0 is the value at zero shear and comes from the Carreau data. The shear stress, $\tau_{1/2}$, at which $\eta=\eta_0/2$ is simply $\tau_{1/2}=\eta_0 u_{z1/2}/2$ where $u_{z1/2}$ is the shear rate where $\eta=\eta_0/2$. Since the Carreau parameters have already

TABLE I. Power law, Carreau, and Ellis parameter values for various fluids.

	Power law		Carreau fluid			Ellis fluid	
Material	n_p	K	n_c	λ	η_0	α	$\tau_{1/2}$
Polystyrene	0.39	3.5×10^5	0.4	46.4	4×10^6	3.2	1.26×10^5
Aluminum soap	n_c	68.07	0.2	1.41	89.6	5.3	69.19
Polyethylene oxide	n_c	13.787	0.4133	1.1876	15.25	2.7	19.918
Hydroxylethycellulose	0.5088	0.84	n_p	0.0664	0.22	2.073	4.93
Blood	0.6	0.035	0.3568	3.313	0.056	3.4	0.026

been adjusted to provide a good fit to the data, we take $u_{z1/2}$ from the Carreau model. Hence we are only left with one parameter, α, to adjust in the Ellis model. This is done by a bisection method to match the slopes in the transition region. The third data set is taken from experimental results reported by Carreau *et al.* [[30], Fig. 7] on 3% solutions of polyethylene oxide in water. The experimental data clearly show the Newtonian plateau for $\dot{\gamma}<1$; for $\dot{\gamma}>5$ the data approximate very well to a straight line (both axes are logarithmic). The power law and Ellis parameters are obtained as described above.

Bird [3, pp. 209–212] gives power law and Ellis model parameters for aqueous solutions of 0.5% hydroxyethylcellulose; this provides the fourth data set. The Carreau parameters are obtained by taking η_0 from the Ellis data, n_c from the power law data, and $\lambda=(K/\eta_0)^{1/(n-1)}$. The final data set is for blood. Many models have been proposed to describe the rheology of blood, yet none are universally accepted. The experimental data in Chien [31] appear to indicate a classical structural viscosity model. The power law and Carreau parameters are taken from [7], which also gives parameters for a range of other models (but not Ellis). The Ellis parameter values are obtained from the Carreau parameters.

Figures 1(a)–1(d) show a comparison of the viscosities predicted by the above models and parameter values for polystyrene, aluminum soap, hydroxyethylcellulose, and blood. The solid line is the Ellis model, the dashed line Carreau, and the dash-dot line power law. We omit polyethylene oxide to save space and also because the correspondence between models is similar to that of aluminum soap, i.e., they all agree well in the shear thinning region and the Ellis and Carreau models only have a slight difference in the transition to the Newtonian plateau.

All the figures show that for low shear rates the power law model significantly overpredicts the viscosity. Figure 1(a) shows the viscosity variation for polystyrene. In this case all parameter values are taken from the literature and, while the agreement is good for low shear, $u_z\in[0.06,1]$, all the curves have a different slope for high shear and consequently diverge. Figures 1(b) and 1(c) both show very good agreement with Ellis and Carreau models; obviously this is expected since for aluminum soap the Ellis parameters have been chosen to obtain good agreement, while for hydroxyethylcellulose the Carreau parameters have been chosen to match the Ellis model. Only in the transition from Newtonian to shear thinning is there a slight difference between the models. For high shear rates the power law model agrees well in both cases, since we have chosen $n_c=n_p$. In Fig. 1(d) the Carreau and power law models show significantly different results, which may be a consequence of different experimental conditions (recall the power law model may give different parameter values depending on the experiment [10]). In [7] it is stated that the Carreau model fits experimental data quite well, so the Ellis model has therefore been chosen to match the Carreau model.

III. FREE SURFACE FLOW OF A FLAT FILM

We consider a film of constant thickness h flowing down a plane inclined at angle θ to the horizontal. The free surface is stress free $\tau=\eta u_z=0$ and a no-slip condition applies on the substrate. The lubrication approximation to the two-dimensional Navier-Stokes equations gives a leading order balance

$$-p_x+\frac{\partial\tau}{\partial z}+\rho g\sin\theta=0,\quad -p_z-\rho g\cos\theta=0.$$

This may be integrated subject to the stress-free condition on the free surface. Since the free surface has a constant height we can set $p=p_a$, where p_a is the ambient pressure at $z=h$. We find

$$\tau=-\rho g\sin\theta(z-h), \tag{4a}$$

$$p=p_a-\rho g\cos\theta(z-h), \tag{4b}$$

where we have used the fact that $p_x=0$ to write the first equation. To proceed further we need to specify a relation between shear stress and shear rate and so must consider the different fluid models. Since our interest lies with the velocity profiles we neglect the pressure expression from now on. Further, for free surface purely gravity-driven flow the velocity gradient u_z is positive everywhere, hence we can neglect the modulus sign in Eqs. (1) and (3).

A. Power law fluid

Substituting for τ from Eq. (1) we find

$$u_z^{n_p}=A_p(h-z),\quad A_p=\frac{\rho g\sin\theta}{K}. \tag{5}$$

This integrates immediately, subject to the no-slip condition, to give the velocity

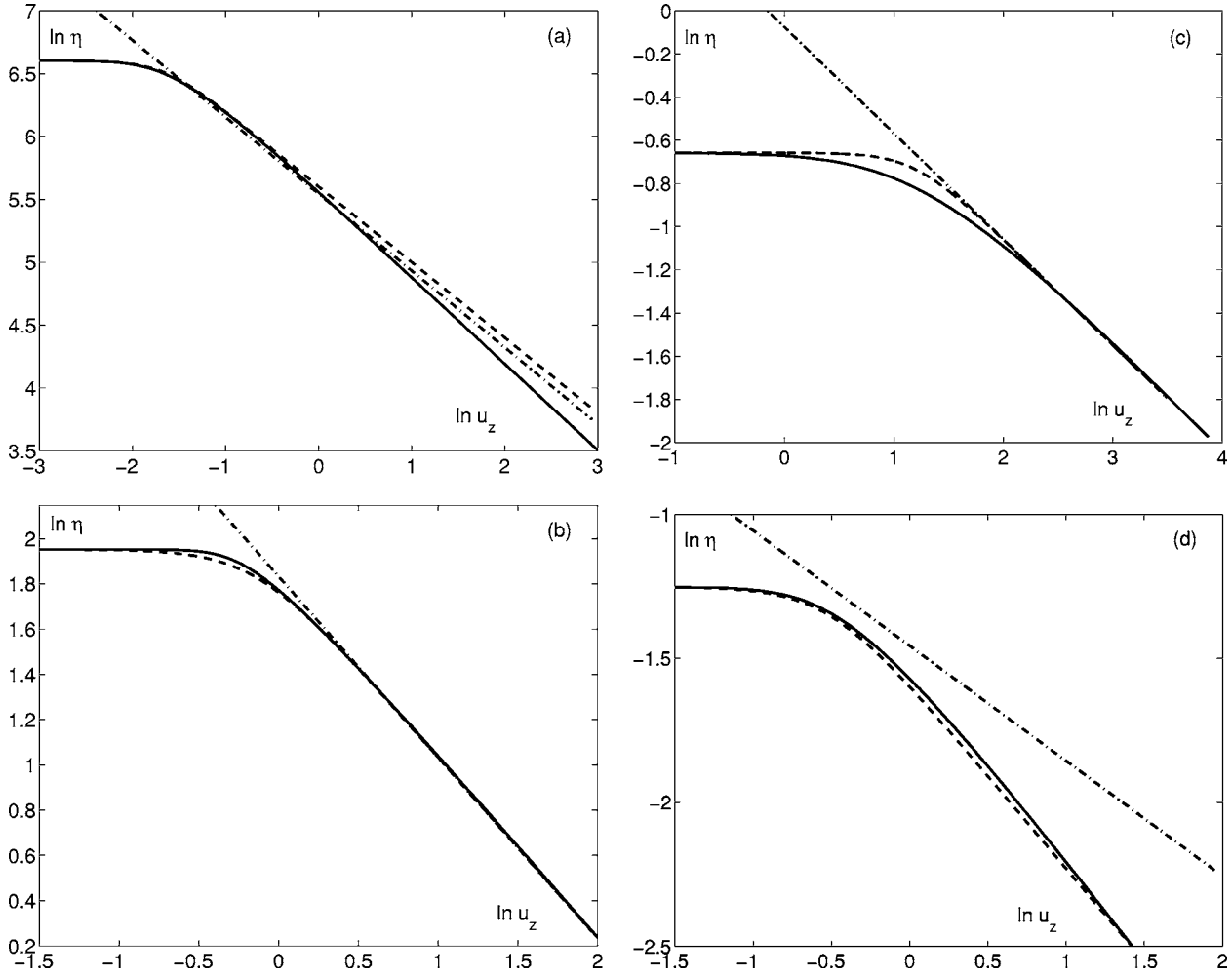

FIG. 1. Comparison of viscosities calculated by the Carreau (dashed), Ellis (solid), and power law (dash-dot) models for (a) polystyrene, (b) aluminum soap, (c) 0.5% hydroxyethylcellulose solution, and (d) blood for the parameter values given in Table I.

$$u = A_p^{1/n_p} \frac{n_p}{n_p + 1} [h^{(n_p+1)/n_p} - (h-z)^{(n_p+1)/n_p}]. \quad (6)$$

Perazzo and Gratton [20,21] consider the flow of a thin layer of power law fluid down a slope. Equation (6) corresponds to their equation with a constant height [see (21, Eq. 13)].

B. Carreau fluid

For the Carreau fluid the velocity in the x direction is determined by

$$(1 + \lambda^2 u_z^2)^{(n_c-1)/2} u_z = A_c (h-z), \quad A_c = \frac{\rho g \sin\theta}{\eta_0}. \quad (7)$$

This cannot be integrated (analytically) further, as in the power law case, and must be treated as a numerical problem.

C. Ellis fluid

Equation (4) provides an expression for τ throughout the film. We may use this to replace τ in Eq. (3). It then follows that

$$u_z = A_c (h-z)\{1 + [A_e (h-z)]^{\alpha-1}\}, \quad A_e = \frac{\rho g \sin\theta}{\tau_{1/2}}. \quad (8)$$

Integrating and applying the no-slip condition gives

$$u = A_c \left(\frac{h^2 - (h-z)^2}{2} + A_e^{\alpha-1} \frac{h^{\alpha+1} - (h-z)^{\alpha+1}}{\alpha+1} \right). \quad (9)$$

A similar expression is given in [10]. Weidner and Schwartz [32] use the Ellis model to describe free surface flow including the effect of surface tension. We will discuss this later.

D. Results

The purpose of this section is to ascertain whether the Ellis model can give similar results to the Carreau model. If so, then we can use Ellis to describe the flow of any fluid which is normally described by a Carreau model. Also we wish to see how well power law fluids compare with the other models.

We will take the Carreau model as our benchmark and so use the viscosity and velocities predicted by this model as correct. Of course there are fluids where the Ellis model

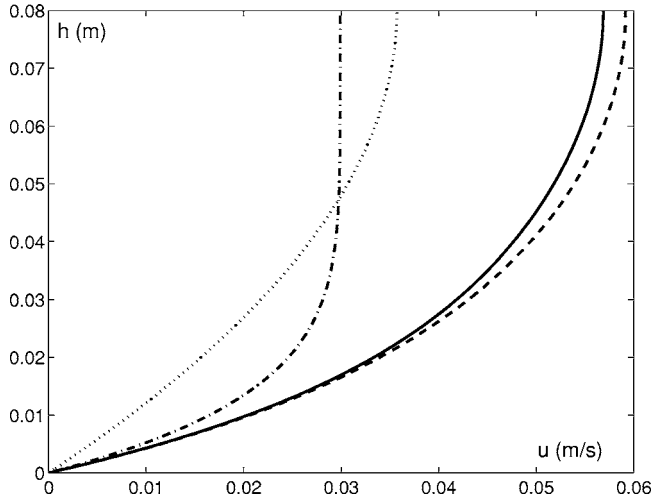

FIG. 2. Comparison of velocities calculated by Carreau (dashed), Ellis (solid), power law (dash-dot), and Newtonian (dotted) models for aluminum soap.

provides a better description; however, if we can make the Ellis results look like the Carreau model results, then we are able to do the opposite. The real question is, then, can the Ellis model match the results predicted by a Carreau model?

We do not present results for free surface flow of molten polystyrene due to its very high viscosity. In this case we would require "films" of the order tens of meters to obtain noticeable flow. Hence, we start with a more practical film of aluminum soap. Figure 2 shows the velocity profiles predicted for Newtonian, power law, Carreau, and Ellis fluids for a film of thickness 8 cm on a slope such that $\rho g \sin\theta = 1000\ \mathrm{kg\ m^{-2}\ s^{-2}}$. As is to be expected from the agreement in Fig. 1 the Ellis and Carreau models lead to very similar velocity profiles with a maximum velocity around 6 cm/s and a maximum of 4% difference. The power law model provides terrible agreement, with a maximum velocity approximately half of that predicted by the Carreau model and even less than the Newtonian result. This is an obvious consequence of the high viscosity prediction. The maximum shear rate is around $2.5\ \mathrm{s^{-1}}$, so, according to Fig. 1(b), most of the flow occurs when the power law model is not appropriate. Decreasing the film height increases the difference between the power law and Carreau models, while the Carreau and Ellis models converge. For $h \leqslant 1$ cm the Carreau, Ellis, and Newtonian models give virtually the same results. The power law model has a maximum velocity less than 0.1% of these other three models. For $h > 20$ cm the power law and Carreau models converge, with a maximum velocity of around 8 m/s. The Ellis model still gives close agreement. However, such a high velocity means this is unlikely to be in a region where the lubrication approximation is still valid. Similar results are found for polyethylene oxide solution.

Now consider Fig. 3(a). This shows the velocity profiles for the different models for a 5 mm thick layer of hydroxyethylcellulose solution, again $\rho g \sin\theta = 1000\ \mathrm{kg\ m^{-2}\ s^{-2}}$. We choose this thickness because it corresponds to a maximum shear rate of around $40\ \mathrm{s^{-1}}$, which places the results in the region of worst agreement between the Ellis and Carreau models (there is around 17% difference in the viscosity predictions). Consequently there is a 27% difference in the maximum velocities. Again the power law fluid shows bad agreement.

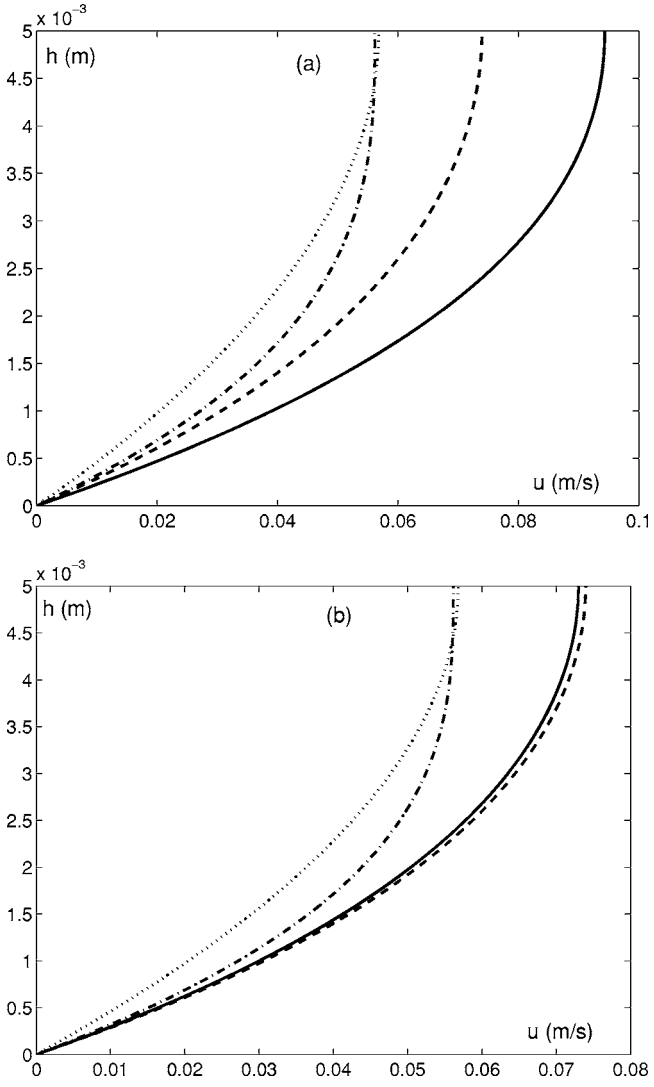

FIG. 3. Comparison of velocities calculated by Carreau (dashed), Ellis (solid), power law (dash-dot), and Newtonian (dotted) models for hydroxyethylcellulose solution with parameter values from (a) Table I and (b) revised values.

The disagreement between Ellis and Carreau might suggest that one of these models is not always appropriate. However, the problem can be remedied. Since we are dealing with thin film, free surface flows we are focusing on flows with relatively small velocities and shear rates. In this case we can drastically improve the correspondence between the Ellis and Carreau models by changing the parameter values. Since we are assuming the Carreau model provides the correct result, we start by taking a model of the form

$$\frac{1}{\eta} = \frac{1}{\eta_0}\left(1 + \left|\frac{\tau}{\beta}\right|^{\alpha-1}\right), \tag{10}$$

i.e., of the same form as the Ellis model but now with a free parameter β as opposed to a shear stress measured at a par-

ticular point for each fluid. If we choose $\alpha=3$ and $\beta=6.63$, then we obtain velocity profiles which match to within 3.4% for a 1 cm thick film (with a maximum velocity of 50 cm/s). When the height is 1 mm the correspondence is within 0.02%. At this thickness the power law model is out by 80%. In effect what we are doing is exchanging the exact correspondence at $\eta=\eta_0/2$ for a better correspondence elsewhere, in particular, for this study, in regions of low shear rate. In general this is likely to result in worse correspondence for the high shear rate region. Figure 3(b) shows the result of applying the modified model to the 5 mm film. Now the maximum difference between Carreau and Ellis is 1.3%.

It is interesting to note that in a study of spin coating Lawrence and Zhou [28] find poor agreement between Newtonian and Ellis models near the axis of symmetry (where the shear rate is low) when $\alpha<3$. The present analysis and the revised parameter values appear in keeping with their findings.

The new parameter values were chosen by calculating the maximum velocity predicted by Carreau and then substituting this into (9) (with $z=h$). This is carried out for a number of film heights, so we are left with a set of equations to solve for α and $A_e=\rho g \sin\theta/\beta$. The values $\alpha=3$ and $\beta=6.63$ are an average of the results obtained.

The viscosity curves for blood, Fig. 1(d), show that the power law model predicts a very different viscosity to the Carreau model. The Ellis model has already been chosen to give good agreement. If we calculate velocity profiles using the tabulated values, we find, as expected, terrible agreement between Carreau and power law for all film thicknesses. This is easily improved for thick films (assuming Carreau gives the correct fit) by choosing $n_p=n_c$ and $K=0.026$. For thin films the agreement will always be bad.

In answer to the questions posed at the start of this section, first we can get good agreement between Carreau and an Ellis-type model (if not strictly an Ellis model). Hence we may proceed to more complex problems using an Ellis-type model, secure in the knowledge that we will obtain results similar to if we had used the Carreau model, provided the shear rate is within the region of applicability.

The power law model, as expected, showed poor correspondence with the other models when the shear rate was low and it should therefore only be trusted in situations where the shear rate is high enough for the flow to remain within the power law regime for most of the region. To be more precise, if we require the power law flux to be within r% of the Ellis model flux, then the flow must satisfy

$$A_p^{1/n_p}\frac{n_p}{2n_p+1}h^{(2n_p+1)/n_p}=\left(\frac{100-r}{100}\right)A_c\left(\frac{h^3}{3}+A_e^{\alpha-1}\frac{h^{\alpha+2}}{\alpha+2}\right).$$

Note that, since the power law flux should always be lower than the Ellis or Carreau prediction we need only take $(100-r)$% rather than $(100\pm r)$%.

IV. FLOW IN A CHANNEL

Obvious industrial situations where the flow of a thin film in a confined channel occurs are flow in a bearing, extruder, or blade coating. The flow of a power law fluid in a channel has been investigated by many authors, see [22–24]. In particular [24] gives a comprehensive overview of research into the problem. Pressure-driven flow of an Ellis fluid between two parallel plates is discussed in [3, pp. 217–218], [10].

In this situation the flow is subject to no-slip at the top and bottom surfaces. The driving forces are pressure gradient and movement of one or both surfaces; without loss of generality we can assume only the lower surface moves. If we denote the velocity of this surface by W, then our boundary conditions are

$$u|_{z=0}=W, \quad u|_{z=h(x)}=0.$$

A. Power law fluid

For this problem we take a different route to the method of [24]. We use a method that is simpler, avoiding the difficulties with modulus signs, but not as comprehensive. To do this we consider situations where there is at most one turning point in the velocity profile within the channel. We are therefore unable to deal with situations where there is backflow, in which case the analysis of [24] should be used. However, the following method covers many of the situations likely to be encountered in practice, see [3, pp. 217–218].

For a power law fluid the flow is governed by

$$K|u_z|^{n_p-1}u_z=p_x(z-z_m) \tag{11}$$

where z_m is the coordinate where $u_z=0$. To drive flow in the positive x direction $p_x<0$. If the bottom surface is moving with speed $W>0$ and the top is stationary, then there are two possible scenarios. First, the velocity increases through the film until it reaches a maximum (at $z=z_m$), then decreases. Second, u decreases monotonically (in this case z_m will occur outside of the physical domain). We consider the first case since this covers the second. Also, if the turning point is not within the channel, then the problem of infinite viscosity is not encountered and so this situation will not highlight the perils associated with using the power law model.

When $z<z_m$, then $u_z>0$ and

$$u_z^{n_p}=\left(-\frac{p_x}{K}\right)(z_m-z). \tag{12}$$

Integrating and applying $u(0)=W$ give

$$u=W+\frac{n_p}{n_p+1}\left(-\frac{p_x}{K}\right)^{1/n_p}[z_m^{(n_p+1)/n_p}-(z_m-z)^{(n_p+1)/n_p}]. \tag{13}$$

When $z>z_m$, then $u_z<0$ and

$$(-u_z)^{n_p-1}(-u_z)=(-u_z)^{n_p}=\left(-\frac{p_x}{K}\right)(z-z_m). \tag{14}$$

Integrating and applying $u(h)=0$ give

$$u=\frac{n_p}{n_p+1}\left(-\frac{p_x}{K}\right)^{1/n_p}[(h-z_m)^{(n_p+1)/n_p}-(z-z_m)^{(n_p+1)/n_p}]. \tag{15}$$

The fluid flux in the channel is $Q=Q_1+Q_2$ where

$$Q_1 = \int_0^{z_m} u dz = W z_m + \left(-\frac{p_x}{K}\right)^{1/n_p} \frac{n_p z_m^{(2n_p+1)/n_p}}{2n_p+1}, \quad (16)$$

$$Q_2 = \int_{z_m}^{h} u dz = \left(-\frac{p_x}{K}\right)^{1/n_p} \frac{n_p (h-z_m)^{(2n_p+1)/n_p}}{2n_p+1}. \quad (17)$$

Adding these two equations allows us to obtain an expression for the flux in terms of the pressure gradient

$$Q = W z_m + \frac{n_p}{2n_p+1}\left(-\frac{p_x}{K}\right)^{1/n_p} [z_m^{(2n_p+1)/n_p} + (h-z_m)^{(2n_p+1)/n_p}]. \quad (18)$$

The position where the velocity gradient is zero is determined by continuity of $u(z_m)$:

$$u(z_m) = \frac{n_p}{n_p+1}\left(-\frac{p_x}{K}\right)^{1/n_p} z_m^{(n_p+1)/n_p} + W = \frac{n_p}{n_p+1}\left(-\frac{p_x}{K}\right)^{1/n_p} (h-z_m)^{(n_p+1)/n_p}. \quad (19)$$

For an incompressible fluid the flux must be constant. We consider the case where the flux is prescribed, similar to the method described in [23]. Of course it is possible that the pressure is known at either end of the region not the flux, in which case (18) must be treated as a form of Reynolds equation which is subject to pressure boundary conditions at either end. The flux then becomes a parameter that must be adjusted to allow both conditions to be satisfied.

However, given a flux Q, Eq. (18) determines the pressure gradient as a function of z_m, at any point x [recall $h=h(x)$]. Substituting the pressure gradient into Eq. (19) then gives a single equation for z_m. Once z_m is determined the pressure gradient and hence the velocity are also known. Note, in the case $W=0$, Eq. (19) has the single real solution $z_m=h/2$ and we only need solve (18) to determine p_x. If $n_p=1$ and $K=\eta_0$, then this gives $p_x=-12\eta_0 Q/h^3$, which is the classical Newtonian result.

B. Ellis fluid

We carry out a similar analysis for an Ellis fluid. The flow is governed by

$$\eta_0 u_z = p_x (z-z_m)\left(1+\left|\frac{p_x(z-z_m)}{\beta}\right|^{\alpha-1}\right). \quad (20)$$

When $z<z_m$, then $u_z>0$ and

$$\eta_0 u_z = -p_x\left[z_m - z + \left(-\frac{p_x}{\beta}\right)^{\alpha-1}(z_m-z)^{\alpha}\right]. \quad (21)$$

Integrating and applying $u(0)=W$ give

$$u = W - \frac{p_x}{\eta_0}\left[\frac{z_m^2-(z_m-z)^2}{2} + \left(-\frac{p_x}{\beta}\right)^{\alpha-1}\frac{z_m^{\alpha+1}-(z_m-z)^{\alpha+1}}{\alpha+1}\right]. \quad (22)$$

When $z>z_m$, then $u_z<0$ and

$$\eta_0 u_z = p_x\left[z - z_m + \left(-\frac{p_x}{\beta}\right)^{\alpha-1}(z-z_m)^{\alpha}\right]. \quad (23)$$

Integrating and applying $u(h)=0$ give

$$u = -\frac{p_x}{\eta_0}\left[\frac{(h-z_m)^2-(z-z_m)^2}{2} + \left(-\frac{p_x}{\beta}\right)^{\alpha-1}\frac{(h-z_m)^{\alpha+1}-(z-z_m)^{\alpha+1}}{\alpha+1}\right]. \quad (24)$$

Integrating again and adding the expressions for Q_1 and Q_2 give

$$Q = W z_m - \frac{p_x}{\eta_0}\left[\frac{(h-z_m)^3+z_m^3}{3} + \left(-\frac{p_x}{\beta}\right)^{\alpha-1}\frac{z_m^{\alpha+2}+(h-z_m)^{\alpha+2}}{\alpha+2}\right]. \quad (25)$$

This is nonlinear in p_x so, unlike the power law case, we cannot write an explicit expression for p_x in terms of the other variables.

The position where the velocity gradient is zero is again determined by continuity of $u(z_m)$ and reduces to

$$W = \frac{p_x}{\eta_0}\left[\frac{z_m^2-(h-z_m)^2}{2} + \left(-\frac{p_x}{\beta}\right)^{\alpha-1}\frac{z_m^{\alpha+1}-(h-z_m)^{\alpha+1}}{\alpha+1}\right]. \quad (26)$$

From Eq. (26) we can obtain an expression for $(-p_x/\beta)^{\alpha-1}$, which may be substituted into (25) to give a linear equation for p_x, with solution

$$\frac{p_x}{\eta_0} = \frac{W\left(z_m - \frac{\alpha+1}{\alpha+2}\frac{z_m^{\alpha+2}+(h-z_m)^{\alpha+2}}{z_m^{\alpha+1}-(h-z_m)^{\alpha+1}}\right) - Q}{\left(\frac{(h-z_m)^3+z_m^3}{3} - \frac{\alpha+1}{\alpha+2}\frac{z_m^{\alpha+2}+(h-z_m)^{\alpha+2}}{z_m^{\alpha+1}-(h-z_m)^{\alpha+1}}\frac{z_m^2-(h-z_m)^2}{2}\right)}. \quad (27)$$

We can then substitute this back into (26) to obtain a rather unpleasant equation that requires solving numerically for z_m.

When $W=0$ Eq. (26) has the single solution $z_m=h/2$ and Eq. (25) determines p_x. The Newtonian limit is retrieved when $\beta\to\infty$.

C. Results for channel flow

In the following we consider only the simplest case, where $W=0$, since this sufficiently illustrates the general form of results. We fix Q and calculate the velocity and viscosity profiles. The pressure gradient to drive this flow is then given by either Eq. (18) or (25).

The velocity and viscosity profiles for molten polystyrene are shown in Fig. 4. The parameters have been changed from

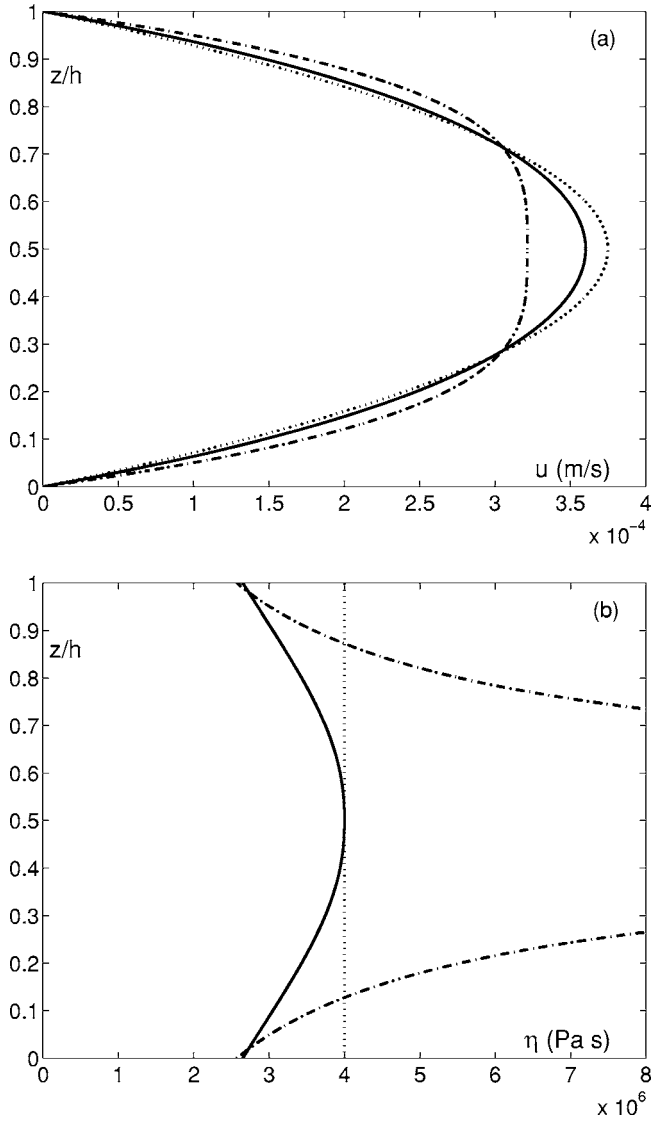

FIG. 4. (a) Velocity profiles predicted by Ellis (solid line), power law (dash-dot line), and Newtonian (dotted line) models for molten polystyrene with $h=5$ cm, $L=50$ cm, and $Q=1.25\times10^{-5}$ m^3 s^{-1} and (b) corresponding viscosity.

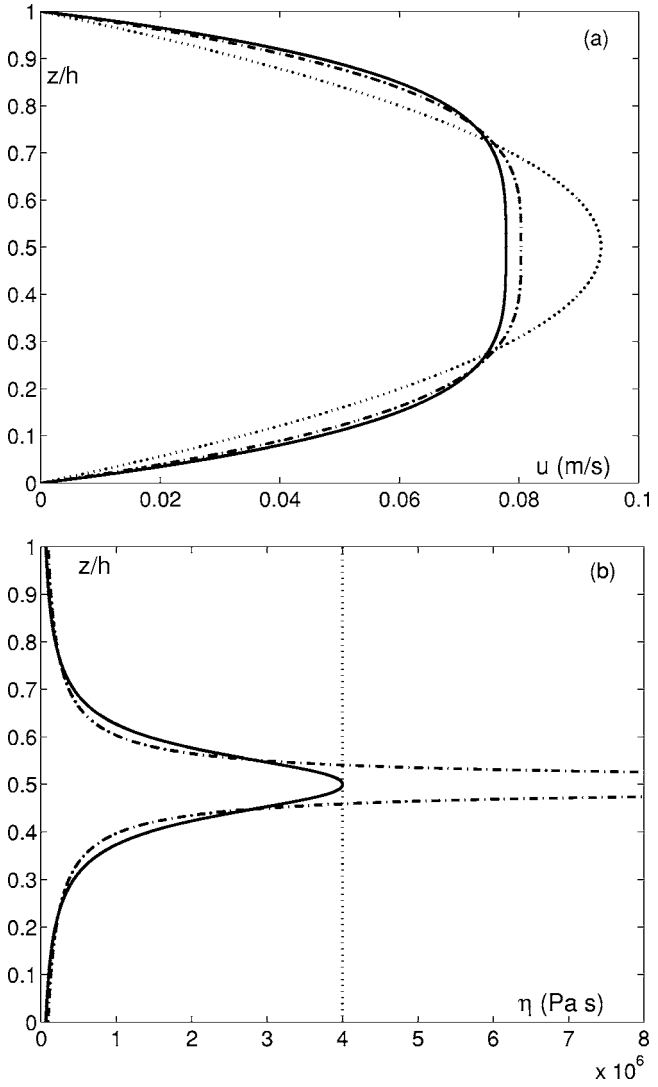

FIG. 5. (a) Velocity profiles predicted by Ellis (solid line), power law (dash-dot line), and Newtonian (dotted line) models for molten polystyrene with $h=5$ cm, $L=50$ cm, and $Q=0.0031$ m^3 s^{-1} and (b) corresponding viscosity.

those quoted in Table 1 of [4] to $n_c=n_p=0.4$ and $K=\eta_0\lambda^{n_c-1}$. This makes the power law curve identical to Carreau for $u_z>0.1$. We also use the modified version of the Ellis law, with $\alpha=3.164$ and $\beta=1.373\times10^5$. These values result in close agreement with Carreau for $u_z<10$; previously the models diverged for $u_z>0.5$. For this simulation the flux is $Q=1.25\times10^{-5}$ m^3/s. The shear rate reaches a maximum of around 0.05 s^{-1} at the channel walls, so from Fig. 1(a) it is clear we are operating around the transition region for the viscosity models. The Ellis and Newtonian velocities are relatively similar and the power law shows significant flattening in the central region, where it approaches plug flow. Since we have fixed the flux as the same for each fluid we should not be surprised at how close the profiles are. However, it takes different pressure gradients to drive each one. We can see from the viscosity curves that the power law fluid has a high viscosity for much of the domain, the Newtonian is next highest, and the Ellis model ranges between $0.7\eta_0$ to η_0. The pressure gradient to drive the Newtonian fluid is 4.8×10^6 Pa/m, for the power law fluid it is 4.6×10^6 Pa/m, and for the Ellis it is 3.8×10^6 Pa/m. Since we know we are in a regime where the Ellis model is close to the Carreau one (which we take as our benchmark) we can see that the pressure gradient driving the power law fluid is out by around 22%. The discrepancy increases as the flow rate decreases. For example, if we decrease the flux by a factor of 2 the power law pressure gradient is out by 60%. Increasing the flow rate causes the Ellis velocity profile to flatten out at the center, becoming more like the power law fluid. This is shown in Fig. 5. Here we have a flux of 0.0031 m^3/s; the maximum shear stress is around 10 (recall the viscosity models diverged past $u_z=10$). The pressure gradient required to drive the Ellis fluid is 3.54×10^7 Pa/m; the power law is 18% higher, while the Newtonian fluid is out by a factor of 100. Given the close correspondence between the Ellis and power law viscosities over much of the channel, it

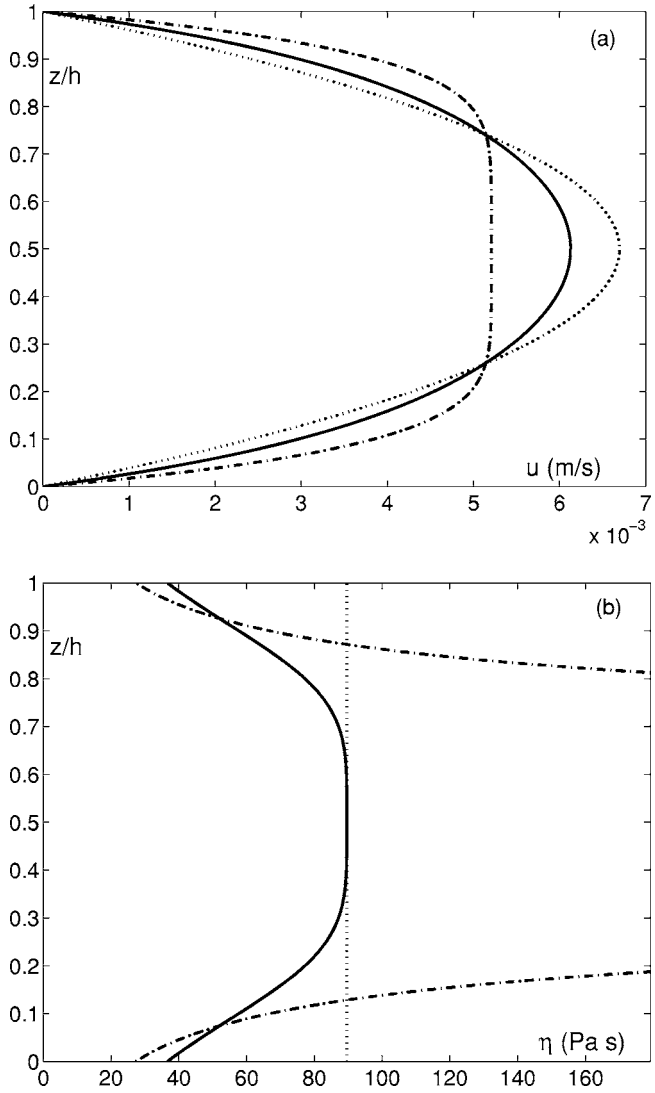

FIG. 6. (a) Velocity profiles predicted by Ellis (solid line), power law (dash-dot line), and Newtonian (dotted line) models for aluminum soap with $h=2$ cm, $L=2$ cm, and $Q=8.9\times10^{-5}$ m^3 s^{-1} and (b) corresponding viscosity.

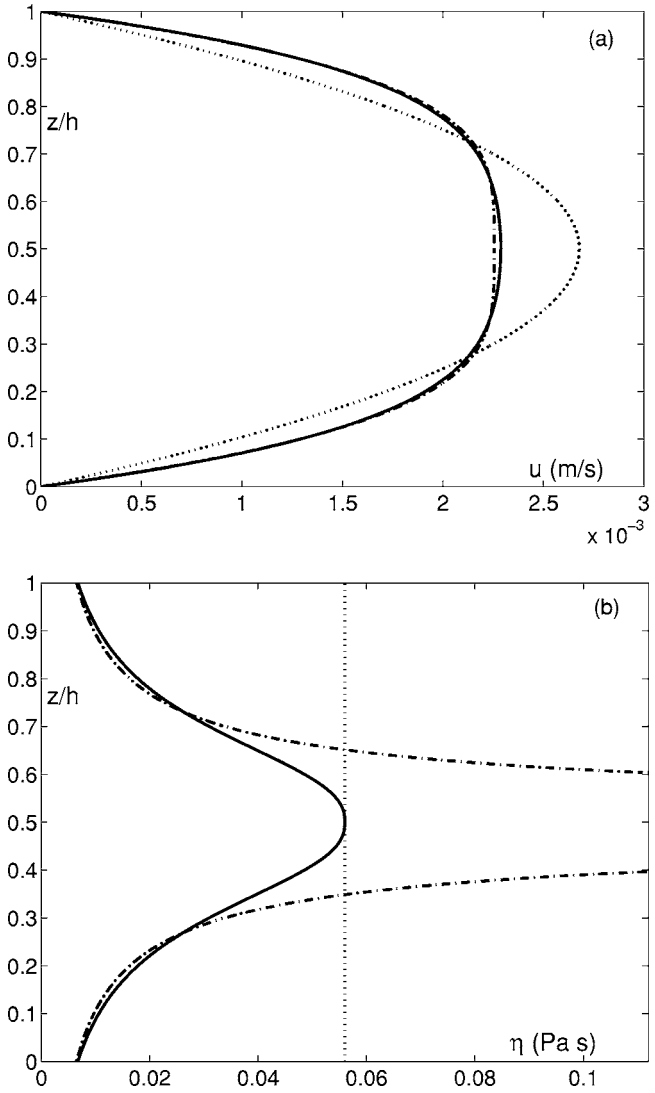

FIG. 7. (a) Velocity profiles predicted by Ellis (solid line), power law (dash-dot line), and Newtonian (dotted line) models for blood with $h=2$ mm, $L=4$ cm, and $Q=3.6\times10^{-6}$ m^3 s^{-1} and (b) corresponding viscosity.

is surprising that there is such a large difference in pressure gradient. Clearly, the central regime where $\eta_p\to\infty$ has a significant effect on the flow.

We show an example for aluminum soap in Fig. 6. The general conclusions are the same as for molten polystyrene. At low shear rates the power law model requires a much higher pressure gradient to drive the flow than the other two models. As the flux increases the power law and Ellis models converge. The Ellis model profile becomes less like the Newtonian parabola and flattens in the center. The result shown in Fig. 6 is for a moderate shear rate, $u_z\sim3$. This is around the region where the viscosities diverge in Fig. 1(b), so we would expect a great difference in the viscosity variation through the profile. This can be seen in Fig. 6(b). However, in this case, considering the large viscosity difference over most of the channel, the pressure gradients are quite close. For the Ellis fluid it is around 7.5×10^3, for the power law it is only 14% higher. The Newtonian pressure gradient is out by a factor of 2.

Finally, consider the flow of blood. The Ellis and Carreau model parameters have already been chosen to give good agreement. The power law parameters are changed to $n_p=n_c=0.3568$ and $K=0.0259$. The general conclusions are the same as for the previous cases. A typical result is shown in Fig. 7. This case has a maximum shear rate, $u_z\sim10$ s^{-1}, which is well into the region of correspondence between Ellis and power law behavior. In the central region, $z\in[0.3,0.7]$, the shear rate is $O(1)$ and the viscosities diverge. However, the Ellis and power law velocities are remarkably similar and the applied pressure gradient is within 7%. The Newtonian pressure gradient is out by a factor of 6.

As in the free surface situation we can write down a relation between the fluxes predicted by power law and Ellis models to quantify the error in the power law prediction. The appropriate fluxes are given by Eqs. (18) and (25). So, for a given pressure gradient we can determine when the power law flux differs from the Ellis flux by r% through the relation

$Q_p=(100-r)Q_e/100$. Note, except in the case where $W=0$, the point z_m does not necessarily coincide for each model and must therefore be calculated separately.

V. FREE SURFACE FLOW WITH SURFACE TENSION

Finally, we briefly describe how the free surface flow equations may be modified to include surface tension.

Now we assume that the film is not flat and modify Eq. (4b) to give

$$p_x = \cos\theta h_x - \sigma h_{xxx}, \tag{28}$$

where σ is the surface tension. Following standard thin film theory [1,2] we will arrive at a mass balance of the form

$$\frac{\partial h}{\partial t} + \frac{\partial Q}{\partial x} = 0, \tag{29}$$

where the flux depends on the fluid in question.

For both power law and Ellis fluids the velocities are the same as given previously by Eqs. (6) and (9), provided the A terms are modified to include the pressure gradient (28),

$$A_p \to \frac{\rho g \sin\theta - p_x}{K}, \quad A_c \to \frac{\rho g \sin\theta - p_x}{\eta_0},$$

$$A_e \to \frac{\rho g \sin\theta - p_x}{\beta}.$$

The appropriate fluxes to substitute into Eq. (29) are

$$Q_p = \frac{A_p h^{(2n_p+1)/n_p}}{2n_p+1}, \quad Q_e = A_c\left(\frac{h^3}{3} + A_e^{\alpha-1}\frac{h^{\alpha+2}}{\alpha+2}\right).$$

A classic problem in thin film theory is the stress singularity that occurs at the moving contact line with a Newtonian fluid. This is the physical manifestation of the contradictory boundary conditions which require the fluid velocity to be zero on the substrate while the free surface is in motion, even where the free surface height tends to zero. Numerical studies on both power law and Ellis fluids in the presence of a moving contact line do not show this stress singularity [12,14,32]. Presumably this occurs because as the stress increases the viscosity decreases and theoretically at infinite shear stress the viscosity is zero. The balance between these two effects results in the removal of the singularity.

VI. CONCLUSION

It is well known that power law fluids are far from ideal when modeling fluid flow at low shear rate. However, since an attractive mathematical model may be obtained, their use is widespread in thin film flow. One of the main purposes of this paper was therefore to investigate how appropriate the use of power law fluids is when dealing with thin film flows where the shear rate becomes zero. A second aim was to present an alternative form that still permits analytical progress. To achieve these aims we chose the Carreau model as our benchmark, since this provides a good approximation to the viscosity of a large number of non-Newtonian fluids.

First, the viscosity was calculated for a number of standard fluids. Power law, Ellis, and Carreau models were compared. This allowed us to adjust published parameter values to obtain a good correspondence with Carreau (over the appropriate region of parameter space) and hence lead to a better comparison of the flow in subsequent sections. The Carreau and Ellis models do not always coincide around the transition region from Newtonian to power law behavior. It was shown that this problem may be overcome by a slight modification to the model. This modification is of particular use to the present study where low shear rates are of interest, although, in general, it will provide worse agreement at very high shear rates.

The results for free surface flow show clearly that when the shear rate is low, the power law model can give wildly inaccurate results. The (modified) Ellis model led to very similar results to Carreau and so it appears that this type of law is appropriate for thin film flows. Of course a truncated power law model [3, p. 209], [15] would give better results than a straight power law model, however, the objections concerning the parameter value estimation still hold and, unless there was a very sharp transition region, there would still be poor agreement around the critical shear rates. Further, a cutoff model requires the use of different equations in different regions and the user must keep track of when to switch. Hence the simplicity of the single power law equation is lost.

Having shown the Ellis model provides very similar results to Carreau, we subsequently dropped the Carreau model when analyzing channel flow. In this case it was shown that for a fixed flux the power law model could require a much higher pressure gradient to drive the flow. Conversely, a fixed pressure gradient would lead to different fluxes between power law and Ellis models. In [4, p. 966] it is stated that in most industrial polymer processing applications the shear rates fall within the domain of the power law regime. However, in channel flow this may be just at the walls and certainly cannot be true throughout the channel. The results shown in Sec. IV C demonstrate that even when the shear rate is relatively high at the wall, the presence of the central, low shear rate region can significantly affect the pressure gradient or flux.

To summarize, clearly great care should be exercised when applying the power law model, particularly when the shear rate is low. Sensibly, it should only be used in situations where the majority of the flow is subject to a shear rate significantly above the transition range. A comparison of the fluxes predicted by the different models, as discussed at the end of Secs. III D and IV C, seems a reasonable way to carry out this check.

The power law model has been preferred over other viscosity models by theoreticians due to the simplicity of the resultant flow equations. However, we have shown that the power law model can give very inaccurate results when applied to physically realistic flows, particularly when the shear rate is low. The Ellis model (or the modified version) has been shown to agree well with Carreau; it also leads to relatively simple governing equations and should provide plenty of questions to satisfy even the most ardent theoretician.

[1] T. G. Myers, SIAM Rev. **40**, 441 (1998).
[2] A. Oron, S. H. Davis, and S. G. Bankoff, Rev. Mod. Phys. **69**(3), 931 (1997).
[3] R. B. Bird, R. C. Armstrong, and O. Hassager, *Dynamics of Polymeric Fluids, Vol. I—Fluid Mechanics* (John Wiley & Sons, New York, 1977).
[4] N. P. Cheremisinoff, ed., *Encyclopedia of Fluid Mechanics, Volume 7* (Gulf Publishing, Houston, 1988).
[5] G. T. Helleloid, Morehead Elect. J. Applicable Maths. **1**, 1 (2003).
[6] "The viscous characteristics of channel bottom muds," Dredging Research Technical Notes, DRP-2-04, July 1992.
[7] R. M. Johnston, P. R. Johnston, S. Corney, and D. Kilpatrick, J. Biomech. **37**, 709 (2004).
[8] I. Machac, B. Siska, and Z. Lecjaks, Chem. Papers **53**(6), 390 (1999).
[9] A. V. Wilchinsky and D. L. Feltharn, Eur. J. Mech. B/Fluids **23**(5), 681 (2004).
[10] S. Matsuhisa and R. B. Bird, AIChE J. **11**(4), 588 (1965).
[11] A. Acrivos and E. E. Petersen, J. Appl. Phys. **31**(6), 963 (1960).
[12] L. Ansini and L. Giacomelli, Nonlinearity **15**(6), 2147 (2002).
[13] S. I. Betelu and M. A. Fontelos, Appl. Math. Lett. **16**(8), 1315 (2003).
[14] S. I. Betelu and M. A. Fontelos, Math. Comput. Modell. **40**(7–8), 729 (2004).
[15] A. Carre and P. Woehl, Langmuir **18**(9), 3600 (2002).
[16] J. C. Flitton and J. R. King, J. Eng. Math. **50**(2–3), 241 (2004).
[17] J. Gratton, F. Minotti, and S. M. Mahajan, Phys. Rev. E **60**(6), 6960 (1999).
[18] H. Pascal, Int. J. Eng. Sci. **29**, 1307 (1991).
[19] J. P. Pascal and H. Pascal, Int. J. Non-Linear Mech. **30**(4), 487 (1995).
[20] C. A. Perazzo and J. Gratton, Phys. Rev. E **67**, 016307 (2003).
[21] C. A. Perazzo and J. Gratton, J. Non-Newtonian Fluid Mech. **118**(1), 57 (2004).
[22] A. F. Elkouh and D. F. Yang, Trans. ASME, J. Tribol. **113**(3), 428 (1991).
[23] M. W. Johnson and S. Mangkoesoebroto, Trans. ASME, J. Tribol. **115**(1), 71 (1993).
[24] A. B. Ross, S. K. Wilson, and B. R. Duffy, Phys. Fluids **11**(5), 958 (1999).
[25] A. G. Emslie, F. T. Bonner, and L. G. Peck, J. Appl. Phys. **29**(5), 858 (1958).
[26] S. A. Jenekhe and S. B. Schuldt, Ind. Eng. Chem. Fundam. **23**(4), 432 (1984).
[27] S. Fomin, J. Watterson, S. Raghunathan, and E. Harkin-Jones, Theor. Comput. Fluid Dyn. **15**(2), 83 (2001).
[28] C. J. Lawrence and W. Zhou, J. Non-Newtonian Fluid Mech. **39**, 137 (1991).
[29] D. V. Boger, Nature (London) **265**, 126 (1977).
[30] P. J. Carreau, D. C. R. de Kee, and R. P. Chabra, *Rheology of Polymeric Systems: Principles and Applications* (Hanser/Gardner Publications, Cincinnati, 1997).
[31] S. Chien, Science **168**, 22 (1970).
[32] D. E. Weidner and L. W. Schwartz, Phys. Fluids **6**(11), 3535 (1994).